Influence of Chain Length and Salt Concentration on Block Copolymer Micellization

Timo Rager, Wolfgang H. Meyer,* and Gerhard Wegner

Max-Planck-Institut für Polymerforschung, Ackermannweg 10, 55128 Mainz, Germany

Mitchell A. Winnik

Department of Chemistry, University of Toronto, Toronto, Ontario, Canada M5S 3H6

Received December 18, 1996; Revised Manuscript Received June 6, 1997⊗

ABSTRACT: Three pairs of end-labeled poly(acrylic acid-*b*-methyl methacrylate) block copolymers were synthesized to study micelle formation in water by nonradiative energy transfer (NRET). One member of each pair contained naphthalene as the donor chromophore at the poly(methyl methacrylate) (PMMA) chain end, and the other, pyrene as the acceptor. The highest molecular weight sample (70 MMA units) formed micelles at the lowest concentrations we could examine, 0.1 mg/L, and did not undergo chain exchange on the time scale of weeks. This polymer forms micelles when the solid sample is treated with 1 equiv of NaOH in water, but the mechanism of micelle formation appears to involve fragmentation of the polymer powder instead of an association of single block copolymer chains. The samples with 40 or 20 MMA units are largely dissociated in pure water, and micelle formation is only slightly increased at higher polymer concentration. No cmc could be observed. However, for these samples addition of small amounts of salt (NaCl) strongly increases the polymer aggregation. The presence of salt also slows down the exchange rate of polymers among the micelles.

Introduction

Over the past 10 to 15 years, the aggregation behavior of amphiphilic block copolymers in aqueous solution has been studied for several polymer systems. Issues investigated include the form and size of the micelles, the critical micelle concentration (cmc),[1−10] and the dynamics of chain exchange between micelles.[10−13] Many of these studies have involved fluorescence techniques, either through the addition of fluorescent dyes as probes to the block copolymer solutions,[1−7] or by covalently attaching the fluorophore directly to the polymer.[8−11]

These various studies indicate a behavior of the block copolymers which is reminiscent of that of low molecular weight surfactants, and as a consequence the principle of closed association,[14] which describes the behavior of low molecular weight surfactants, is generally accepted to apply to block copolymer systems as well. However, there exist some problems in characterizing block copolymer aggregation. The cmc values are often extremely low (in the range of mg/L) and close to or even below the limit of experimental detection. In some cases different measurements have lead to contradictory cmc values for the same sample.[6,7]

Another problem often encountered with block copolymers in water is the difficulty to dissolve the polymers directly in water. Whereas some hydrophilic polymers like the Pluronics[4−6] disperse readily in water, other block copolymers (containing a polystyrene block in most of the cases) need to be heated or require long stirring times to get clear solutions.[1,2,15] Sometimes, lengthy procedures including dialysis are necessary to obtain uniform micelles,[8,16,17] and in some reports, the authors confined their investigations to mixtures of water with organic solvents to avoid these problems.[10,18,19] These dissolution difficulties may be connected with long hybridization times: In many cases, chain exchange between micelles requires hours.[10,11,13] One indication of slow exchange is the detection of sharp peaks in a gel permeation chromatography (GPC) experiment, indicating no significant exchange on the time scale of the experiment.[2,20] Several authors, including Munk *et al.*[12,13] and Mattice *et al.*[11] have demonstrated that for some block copolymers the chain exchange between micelles is much slower, in the range of days or weeks, or not observable at all. Here it is possible, or even likely, that the micelles are not in their true equilibrium state. Two features are supposed to control the slow rate of exchange in these systems. One is the low solubility of the hydrophobic block in water. In addition, the core material of the micelles may be in its glassy state at room temperature. Thus there is a kinetic as well as a thermodynamic barrier for chains to exit from a micelle.[21]

The objective of this investigation is to examine the association process in water of neutralized block copolymers (sodium salt) of the type poly(acrylic acid-*b*-methyl methacrylate), a system for which very little information is currently available. We are interested in understanding the influences of chain length, polymer concentration, and salt concentration on micelle formation and micellar stability for this system. For most of our experiments, we take advantage of nonradiative energy transfer (Förster energy transfer, NRET) between fluorescent dyes attached to the block copolymer molecules. This technique samples distances in the nanometer range,[22] which corresponds to micellar dimensions. NRET measurements allow us to distinguish between aggregated and molecularly dissolved states of the system and also permit us to examine the exchange process. Here we describe experiments on three pairs of poly(acrylic acid-*b*-methyl methacrylate) block copolymers either donor-labeled with naphthalene (AA-MMA-N) or acceptor-labeled with pyrene (AA-MMA-Py) at the end of the hydrophobic PMMA block.

Experimental Section

Synthesis of End-Functionalized poly(*tert*-butyl acrylate-*b*-methyl methacrylate) (tBA-MMA-F).[23−25] All reactions were performed under vacuum in a glass apparatus

---

* To whom all correspondence should be addressed.

⊗ Abstract published in *Advance ACS Abstracts,* August 1, 1997.

S0024-9297(96)01866-9 CCC: $14.00

equipped with ROTAFLO stop cocks; the reactor was provided with sufficient ground glass joints to put the ampules with reactants directly on it. THF (Riedel-de Haën Chromasolv) was dried with butyllithium/styrene and cryodistilled. The initiator (diphenylhexyl)lithium was prepared by reaction of butyllithium (12 mL, 19.2 mmol, Acros) and diphenylethylene (3.6 mL, 20.4 mmol, Fluka purum) in dry THF (ca. 100 mL) in a glass ampule under nitrogen. Its approximate concentration was determined by a test polymerization of methyl methacrylate (MMA). The monomers (BASF) were dried by cryodistillation in the presence of triethylaluminum (15% in hexane, Fluka purum);[26] *tert*-butyl acrylate (tBA) was subsequently diluted to about the threefold volume with dry THF. In the reactor, first lithium chloride (0.8 g, 19 mmol, Aldrich 99.99+%) was dried by heating under vacuum. Then dry THF (approximately 400 mL) was cryodistilled to the reactor and initiator (22.4 g, ca. 3 mmol) was added from the ampule. After the reaction mixture was cooled to about −70 °C, tBA (18.9 g, 147 mmol) was added slowly under vigorous stirring. After 15 min MMA (6.6 g, 66 mmol) was added in the same way. After an additional 15 min, the reaction was terminated by adding a solution in dry THF of 1-(bromomethyl)pyrene (730 mg, 2.5 mmol), which had been synthesized as described in ref 27 and dried under high vacuum at ambient temperature. After 1 h of reaction at −70 °C the remaining active ends were quenched with methanol. Twofold precipitation of the product in methanol/water 2:1 gave 24.5 g (92%) of tBA$_{45}$-MMA$_{20}$-Py (the index indicating the degree of polymerization of the corresponding block). Polymers with a naphthalene-label or without fluorophore were synthesized in the same way by adding a solution of either 2-(bromomethyl)naphthalene (Fluka pract.) or methanol instead of 1-(bromomethyl)pyrene.

Synthesis of End-Functionalized Poly(acrylic acid-*b*-methyl methacrylate) (AA-MMA-F).[18,24] tBA$_{45}$-MMA$_{20}$-Py (20.5 g) was heated for 5 h in dioxane (100 mL, Merck p.a.) with concentrated HCl (12 mL, Riedel-de Haën p.a.) to 85 °C. After cooling, the polymer was precipitated in excess petroleum ether and washed several times with this solvent. Afterward the polymer was redissolved in dioxane and freeze-dried, yielding 15.2 g (100%) of AA$_{45}$-MMA$_{20}$-Py.

Instrumentation. Membrane osmometer, capillary osmometer developed at this institute;[28] vapor pressure osmometer, Wescan Model 232A; gel permeation chromotographer, autosampler waters WISP710B, pump waters 590, UV-detector Soma S3702, RI-detector Erma 7510, software waters GPC 860; NMR spectrometer, Varian Gemini 200; UV spectrometer, Perkin Elmer Lambda 2; titrator, Metrohm Potentiograph E536 and Dosimat 655; fluorescence spectrometer, SPEX fluorolog 2; dynamic light scattering, krypton ion laser (Spectra Physics Model 2025, $\lambda = 647.1$ nm), goniometer ALV-SP81, correlator ALV-3000.

Polymer Characterization. Number-averaged molecular weights (M_n) of the unhydrolyzed polymers were determined either by membrane osmometry in toluene or by vapor pressure osmometry in THF at 30 °C. Block composition and end group analysis were performed by ^{1}H NMR using deuterochloroform (unhydrolyzed polymers) or deuterated methanol (hydrolyzed polymers) as solvent. The fraction of end-group-functionalized polymers was determined by UV absorbance measurements: apparent molecular weights were calculated by comparing the absorption of methanol solutions of the block copolymers with that of known concentrations of 1-(hydroxymethyl)pyrene and 2-methylnaphthalene, respectively, as standards. These values were then related to the M_n values obtained by membrane osmometry or NMR. Gel permeation chromatography (GPC) data were obtained for the unhydrolyzed species in THF. A concentration of about 2 g/L, an injection volume of 100 μL, and a flux of 1 mL/min were used. The signal was monitored simultaneously by UV (340 nm for pyrene, 277 nm for naphthalene) and refractive index detectors. The gel permeation chromatographer was calibrated with PMMA standards. To determine the amount of acid groups, approximately 100 mg of each polymer was titrated potentiometrically (0.1 M NaOH added at a rate of 10 mL/30 min) in 30 mL of a mixture of methanol and water 1:2.[29] The acid content determined in this way was always 10−20% lower than that expected from the ^{1}H NMR analysis of the block composition. Reasons for this are difficulties in determining the end point in the titration of polyelectrolytes[30] and weighing errors due to incomplete removal of solvent from the dry sample.

Sample Preparation. Stock solutions with a concentration of several grams per liter were prepared by direct dissolution of the samples in deionized water (Milli Q) with 1 equiv of NaOH (0.1 M, Merck Titrisol), as determined by potentiometric titration. The samples were heated for about 2 h to 80 °C for complete dissolution. The stock solutions had a pH of about 8. Upon dilution with water and sodium chloride the pH decreased to ca. 6. For the NMR investigations small amounts of these solutions were freeze-dried, and the resulting polymer was redissolved in deuterated water.

One stock solution of AA$_{70}$-MMA$_{70}$ for dynamic light-scattering measurements was prepared by dialysis (Spectrapor 6, MWCO = 1000) of a methanolic solution with a concentration of about 2 g/L of polymer in the acid form against a large excess of water for several days. Afterward the polymer was neutralized and dialyzed against 0.1 M NaCl in the same way. Solutions with different polymer concentrations were prepared by dilution with the dialysate. All solutions for light-scattering were filtered several times through a 0.45 μm pore size filter (Millipore) for clarification. The first 2−3 mL was discarded.

Fluorescence Measurements. All spectra were recorded at room temperature from air-saturated solutions in 10 mm × 10 mm quartz cuvettes in the right angle geometry. The excitation wavelength for emission spectra was 288 nm, and the observation wavelength for the excitation spectra, 397 nm. An integration time of 0.5 s/0.5 nm was used, and slit openings of 0.5 mm on the excitation side and 2 mm on the detector side were applied.

To optimize signal detection, in all of our experiments we employed a 5:1 ratio of N- to Py-labeled polymer. Pyrene absorbs some light at the wavelength used to excite naphthalene selectively, and it also has a larger fluorescence quantum yield. If equal amounts of pyrene and naphthalene were present, this would lead to a dominance of the pyrene fluorescence in the spectrum even in the absence of any energy transfer. We found that it was more useful if the state without any energy transfer corresponded to approximately equal fluorescence intensities at the two peak maxima (naphthalene, 336 nm; pyrene, 397 nm). This is attained for a ratio of N-labeled to Py-labeled polymer of 5:1. Under these circumstances, donor−donor transfer may compete with donor−acceptor transfer, even though the critical distance for naphthalene-naphthalene energy migration (7.35 Å) is smaller than the Förster radius for naphthalene−pyrene energy transfer (29 Å).[22c] Since we are using NRET experiments only to determine the conditions under which both donor and acceptor occupy the same micelle, the presence of donor−donor transfer will have no effect on the qualitative conclusions we draw.

All solutions were prepared at least 1 day in advance, even when control experiments showed that shorter times were sufficient to obtain fluorescence spectra that do not change with time.

Dynamic Light-Scattering Measurements. All measurements were performed with 2 cm cylindrical quartz cuvettes at 296 K. Correlation functions were accumulated at five different angles between 30° and 150°.

Results and Discussion

Synthesis and Characterization. The block copolymers were synthesized as depicted in Scheme 1 by anionic polymerization involving initiation with (diphenylhexyl)lithium in the presence of LiCl, followed by sequential addition of *tert*-butyl acrylate (tBA) and methyl methacrylate (MMA).[23,24] The polymers were end-functionalized by reaction of the living anion with a bromomethyl derivative of the chromophore.[25] Afterward the *tert*-butyl esters of the polymer were hydrolyzed with HCl. No signal of the *tert*-butyl ester was visible afterwards in the ^{1}H NMR. We infer that the

Table 1. Characterization of the Samples

	M_n of precursor[b] (g/mol)						x_F[e]	
sample[a]	OM[c]	NMR	GPC(RI)	GPC(UV)	M_w/M_n (GPC)	AA:MMA[d]	UV	NMR
AA_{75}-MMA_{70}-N	16500		18500	17300	1.13	1.1:1	0.8	
AA_{70}-MMA_{70}-Py	15800		18600	16900	1.20	1:1	1	
AA_{70}-MMA_{70}	16000		17800		1.10	1:1		
AA_{35}-MMA_{35}-N	6600	7800	9500	8800	1.13	1:1	0.7	0.6
AA_{40}-MMA_{40}-Py	7300	9200	10200	9200	1.16	1:1	0.9	0.75
AA_{40}-MMA_{20}-N	6300	7800	9200	8300	1.18	2.1:1	0.6	0.45
AA_{45}-MMA_{20}-Py	6300	8000	8600	7800	1.19	2.2:1	0.75	0.6

[a] Subscripts indicate the degree of polymerization of the acrylic acid (AA) and methyl methacrylate (MMA) block, respectively. [b] Poly(*tert*-butyl acrylate-*b*-methyl methacrylate). [c] Membrane osmometry for AA_{75}-MMA_{70}-N, AA_{70}-MMA_{70}-Py, and AA_{70}-MMA_{70}; vapor pressure osmometry for the other samples. [d] Block composition from NMR. [e] Fraction of end-group-functionalized molecules determined by UV and NMR, respectively.

Scheme 1. Synthesis of Poly(acrylic acid-*b*-methyl methacrylate) Block Copolymers

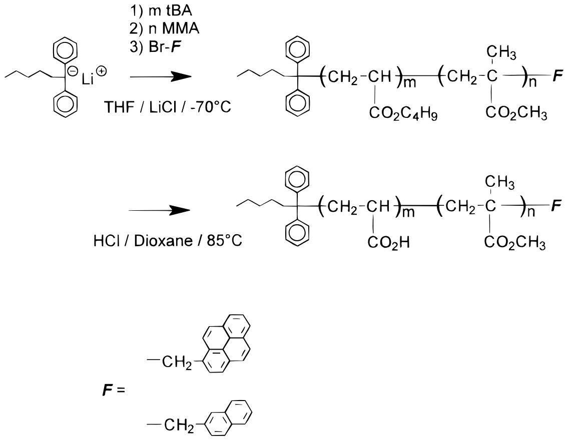

degree of hydrolysis is greater than 95%. In the case of the unlabeled polymer, the reaction was terminated directly with methanol instead of adding the chromophore. Table 1 presents the characteristics of the block copolymers.

Molecular weight determinations by osmometry and GPC were performed with the precursor polymers, i.e., before hydrolysis of the *tert*-butyl esters. Comparison of the methyl protons of MMA and the single main chain proton of either tBA or AA in the ^1H NMR spectrum gave the block composition. For the smaller block copolymers, we were able to observe and quantify the signal from both end groups in the ^1H NMR spectrum. Here the degree of chromophore functionalization x_F and the number-averaged molecular weight (M_n) of the polymer could be calculated. For the larger polymers, the rather broad signals of the end group protons were unsuitable for quantitative integration.

Covalent attachment of the chromophores to the polymer was monitored by GPC using dual detectors. The refractive index (RI) detector monitored the signal due to polymer, and the UV detector, at a wavelength characteristic for each chromophore, monitored the location of chromophore in the system. The good correspondence between both signals indicates that the fluorescent groups are covalently attached and equally distributed over the polymer chains. The small but systematic deviation between the UV and RI signals is due to the fact that the observed intensity is set proportional to the concentration in grams per liter. In the case of end group detection this leads to an underestimation of the high molecular weight fraction. A much smaller error, which should give a displacement of the molecular weight in the opposite direction, will be due to the incomplete labeling, which leads to a mixture of two kinds of polymers, from which only one part is detected by UV. In the case of the naphthalene-labeled polymers a small amount (less than 5% of the signal intensity) of low molecular weight impurities was also detected by UV.

Chromophore content in the hydrolyzed polymers was also determined by UV absorption measurements using 1-(hydroxymethyl)pyrene and 2-methylnaphthalene as model compounds. Apparent M_n values calculated in this way were compared with values obtained from membrane osmometry or NMR to obtain the degree of labeling x_F. The agreement with the degree of labeling determined exclusively by ^1H NMR is reasonable (Table 1) and assumes that the molar extinction coefficients of the model compounds are the same as those of the chromophores attached to the polymers. In any case, the interpretation of the experiments reported below does not depend on 100% functionalization of the chain ends.

It is important to note that the poly(acrylic acid) chains in these diblock copolymers carry a hydrophobic end group at the hydrophilic end, the diphenylhexyl unit from the initiator (see Scheme 1). It is possible that the hydrophobic nature of this end group could influence the behavior of the system in aqueous solution. To the extent that these groups act as sticky ends in water, one might think of our samples as A-B-C triblock copolymers.

Sample Preparation. None of our block copolymers in the protonated form could be dissolved directly in water, but they are soluble in the presence of base. In this respect they differ from higher molecular weight PAA-PMMA block copolymers or PAA-PMMA samples with a higher proportion of PMMA which cannot be dissolved directly in water even in the presence of base.[31] Our experiments are exceptionally sensitive to excess salt in the solution (see below): In order to maximize the solubility of the polymer and yet have a minimum amount of salt in the solution, we wanted to avoid adding excess NaOH to the block copolymer. To attain this, the block copolymer samples were neutralized with 1 equiv of NaOH, as determined from the inflection point of a potentiometric titration curve. The inflection point coincided with the maximum in viscosity of the solution, indicating an optimum between neutralization and excess salt.

Solution Behavior of AA_{70}-MMA_{70}-Py/AA_{75}-MMA_{70}-N in Water. Solutions prepared from the pair of block copolymers containing 70 MMA units showed different fluorescence behavior depending upon how the samples were prepared. When the two polymers (protonated form) as powders were dissolved in aqueous base in separate flasks and mixed afterward (Figure 1, method A), no energy transfer could be observed, even

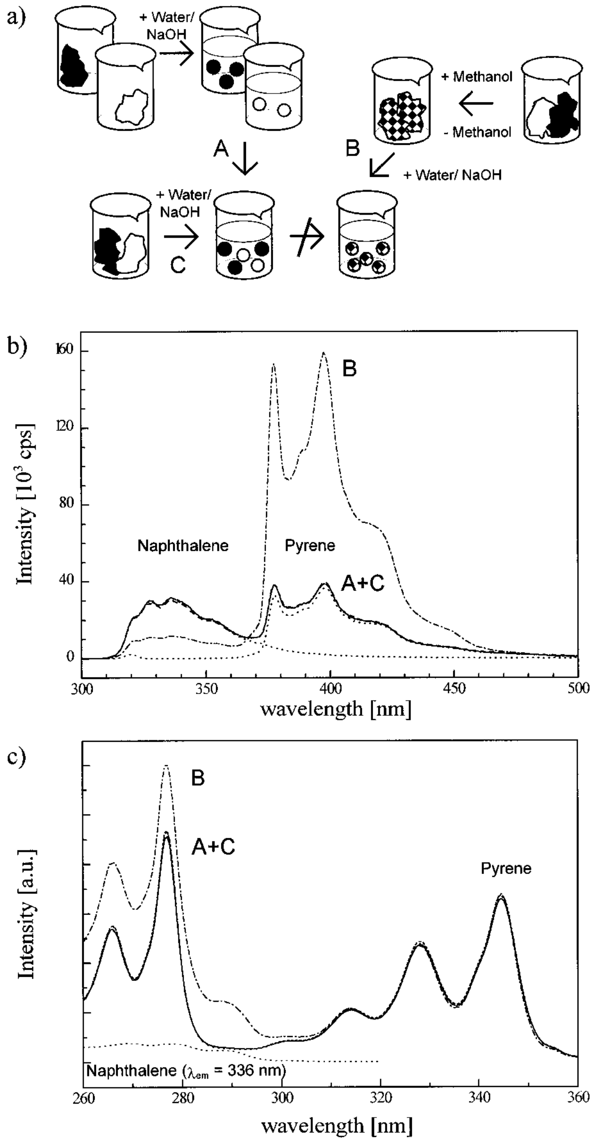

Figure 1. Different preparation pathways (a) lead to solutions of AA_{70}-MMA_{70}-Py/AA_{75}-MMA_{70}-N with different emission spectra (b) and excitation spectra (c). A (—): Dissolution of the two block copolymers (protonated form) in separate flasks with water/NaOH and subsequent combination of the two solutions does not give rise to Förster energy transfer. B (-·-·-): Dissolution of the two polymers together in methanol or dioxane, with subsequent drying of the polymer mixture, and redissolution of the powder in water/NaOH gives rise to efficient Förster energy transfer. C (- - -): Dissolution of the two polymer powders in the same flask with water/NaOH leads to almost no Förster energy transfer as in case A. The spectra of separate solutions of the naphthalene- and pyrene-labeled polymer are represented with dotted lines. For all solutions, the concentrations were 40 mg/L for the naphthalene-labeled polymer and 8 mg/L for the pyrene-labeled polymer.

after many weeks at room temperature or after heating for several hours. When the two polymers in the protonated form were first mixed on a molecular level by dissolving them in dioxane or methanol, redried to yield a powder, and then redissolved in alkaline water (method B), a strong increase of pyrene fluorescence at the expense of the naphthalene signal was observed, and at the same time the excitation spectrum showed a contribution of the naphthalene absorption to the pyrene fluorescence. This indicates the presence of both chromophores in the core of the same micelles. This difference in behavior, reflecting different sample preparation conditions (method A and method B), was observed even for very dilute solutions. Even after dilution to 0.1 mg/L, a significant difference in fluorescence behavior was observed, indicating that micelles are still present. Finally, when the N- and Py-labeled polymers were mixed as powders and then dissolved in aqueous base (method C), a solution was obtained with fluorescence characteristics almost identical to those of a solution prepared by method A, with little or no mixing of the two polymers in the same micelle.

From these observations we conclude that the onset of association of these block copolymers is extremely low and beyond our ability to detect it, that no exchange of single chains between the block copolymer aggregates occurs on the time scale of weeks, and that the dissolution of the block copolymer powder sample occurs by a process involving fragmentation of the powder grains into smaller and smaller parts until colloidal dimensions are reached.[15] Almost no chain exchange between micelles takes place during this process. The block copolymer micelles of poly(acrylic acid sodium salt-*b*-methyl methacrylate) containing sufficiently long PMMA blocks behave in water like inert, sterically stabilized colloidal particles.

Dynamic light-scattering measurements on samples of the unlabeled polymer AA_{70}-MMA_{70} in 0.1 M NaCl showed that the dimensions and uniformity of the micelles prepared by direct dissolution in water/NaOH are similar to, but not identical with, those of the micelles obtained by dialysis of the same sample from methanol into water. The hydrodynamic radius (R_h) obtained by measurements at different polymer concentrations and observation angles was 14.0 ± 0.6 nm (direct dissolution) instead of 12.6 ± 0.6 nm (dialysis). For both systems, the correlation functions were fitted to a stretched exponential, and the second exponent of the fitting function was always above 0.97, which indicates within the limits of the method a narrow distribution of particle sizes.

Solution Behavior of Block Copolymers with Shorter Chain Lengths. In contrast to the preceding observations, polymers containing 40 or 20 MMA units in the PMMA block appear to come to thermodynamic equilibrium relatively rapidly in aqueous solution. Pairs of donor- and acceptor-labeled polymers in aqueous solution exhibit identical fluorescence spectra, irrespective of which of the three dissolution pathways (A, B, or C) is employed. This result suggests that single chains of the polymers (unimers) have finite solubility under these conditions. In these samples the ratio of the pyrene fluorescence intensity at 397 nm to the naphthalene fluorescence intensity at 336 nm (I_P/I_N) in dilute solution (less than 50 mg/L) is much smaller than that in the case of the mixed micelles of block copolymers with 70 MMA units, which I_P/I_N is approximately 13 (Figure 1b). As can be seen in Figure 2, in the case of AA_{40}-MMA_{40}-Py/AA_{35}-MMA_{35}-N the I_P/I_N value drops to ca. 2.0. For AA_{45}-MMA_{20}-Py/AA_{40}-MMA_{20}-N, the I_P/I_N ratio is close to unity and therefore almost corresponds to what would be obtained from a superposition of the spectra of two independent solutions of AA_{45}-MMA_{20}-Py and AA_{40}-MMA_{20}-N with the same concentrations (dotted line in Figure 2). This result indicates that, under these conditions, only a minor amount of these block copolymers is present in the aggregated form.

When the polymer concentration is raised, the ratio I_P/I_N increases (filled circles in Figure 2). At the higher

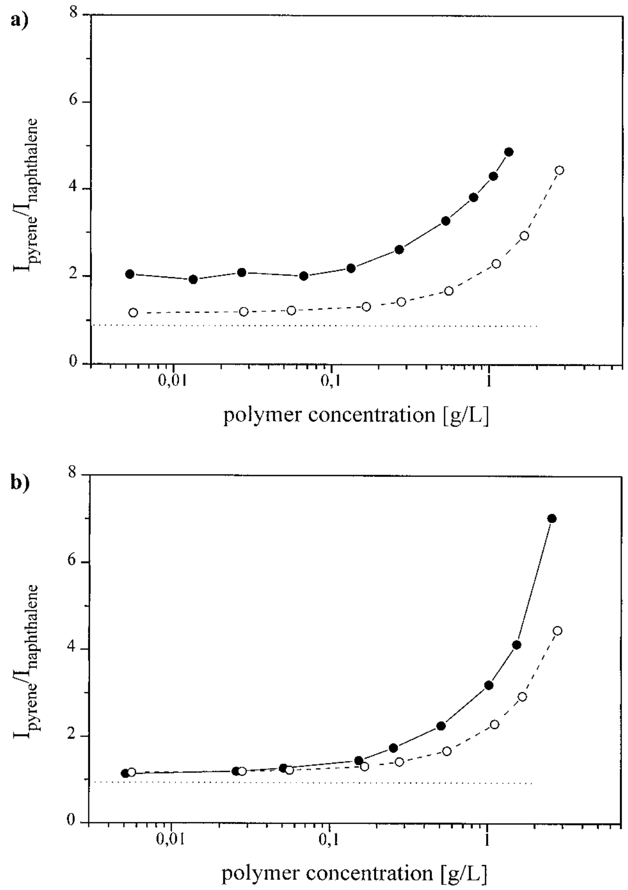

Figure 2. Concentration dependence of the acceptor-to-donor (pyrene/naphthalene) fluorescence intensity ratio (I_P/I_N) for the polymer systems (a) AA_{40}-MMA_{40}-Py/AA_{35}-MMA_{35}-N and (b) AA_{45}-MMA_{20}-Py/AA_{40}-MMA_{20}-N (filled points). The open circles show the relative increase in pyrene fluorescence intensity in a solution of AA_{70}-MMA_{70}-Py/AA_{75}-MMA_{70}-N prepared by method C, where the naphthalene and pyrene are in separate micelles. Here only radiative (trivial) energy transfer can occur. The concentration axis for these solutions has been adapted to give identical pyrene absorption per gram of polymer. The dotted lines parallel to the x-axis represent the I_P/I_N values calculated by the mathematical addition of the fluorescence of the two separate solutions of the low molecular weight block copolymers before mixing.

polymer concentrations, not only does the intensity of the naphthalene fluorescence change but the peak shape changes as well, due to reabsorption of its emitted light by the increasing amount of pyrene present in solution. This effect depends only on the concentration of the acceptor chromophore in solution and not on the distribution of distances between chromophores. Reabsorption of emitted light is referred to by spectroscopists as “trivial energy transfer”, but it is never a small matter to correct the data for this effect. Reabsorption of light depends upon the path length of the light beam in solution. To minimize this effect, these experiments were repeated (not shown here) in the front-face geometry, focusing the excitation and collection optics on the surface of the solution in the cell. Even then, this effect could not be suppressed completely.

In order to analyze the increase in I_P/I_N in more detail, we take advantage of the observation that samples of AA_{70}-MMA_{70}-Py and AA_{75}-MMA_{70}-N do not undergo significant exchange in aqueous solution. A mixture of micelles, where each micelle contains only one of the two chromophores (preparation method A or C), should show the same extent of emission reabsorption as that of the samples with the shorter PMMA blocks at identical chromophore concentration but should exhibit no nonradiative energy transfer. By measuring the concentration dependence of I_P/I_N in this system, only the long range “trivial” energy transfer should be observed and, by taking account of the different chromophore-to-polymer ratio, a baseline for the preceding measurements can be established (the open circles in Figure 2). Figure 2 shows that for both polymer systems the concentration dependence of I_P/I_N is very weak after subtracting the contribution of emission-reabsorption to the signal. A slight increase in I_P/I_N with respect to the new baseline can be discerned at about 100 mg/L, which becomes more pronounced at polymer concentrations above 1 g/L, but this change does not resemble the sharp onset one would expect for a true cmc.

From these observations we draw the curious conclusion that, for the block copolymers with 40 or 20 MMA units, polymer concentration has only a minor influence on the tendency for aggregation. This may be due to the fact that the aggregation strongly depends on the hydrophobic block length and that the transition is therefore smeared out by the polydispersity of the samples. An alternative explanation might be that the preference for a certain aggregation number is much less pronounced for these block copolymers than for low molecular weight amphiphiles and that the micelles can grow continuously up to a maximum aggregation number.

Influence of Salt on Micelle Formation. It is well-known that ionic strength decreases the solubility of nonionic species in water and, by shielding electrostatic repulsion, has a large effect on polyelectrolyte behavior. Several investigations have shown that these principles extend to amphiphilic block copolymers in aqueous solution.[3,19c,32,33] For our samples of the MMA_{70} block copolymers, we observed that they become increasingly difficult to dissolve in aqueous base in the presence of only small amounts of sodium chloride. This behavior is to some extent surprising because postaddition of salt to a preformed micellar solution does not cause precipitation of the polymer. The micelles remain stable for salt concentrations of 0.5 M and higher. Similar behavior was reported by Selb and Gallot for poly(styrene-*b*-vinylpyridinium) block copolymers.[15] The influence of salt on suppressing the solubility of solid block copolymer samples may be related to the fracture mechanism of polymer dissolution described above: In the presence of salt the repulsion between the neutralized, charged acrylic acid blocks may not be sufficient to break up the polymer powder to form micelle-sized aggregates.

To proceed further, we examined the effect of adding salt to the solutions of our block copolymers in water by monitoring its influence on the extent of energy transfer. In the case of AA_{70}-MMA_{70}-Py/AA_{75}-MMA_{70}-N, the change of the fluorescence spectrum by addition of sodium chloride is not very pronounced. Aggregation in this system is nearly complete in pure water, and only minor changes are observed. These we rationalize by recognizing that although the molecular weight distribution of the polymers is quite narrow, there exists a minor part of the block copolymer sample which is soluble in pure water because of its shorter hydrophobic block. If the presence of sodium and chloride ions decreases its solubility, it may become incorporated into the micelles, leading to an increase in NRET.

In the case of the short block copolymers, the influence of added salt on the fluorescence spectra is rather

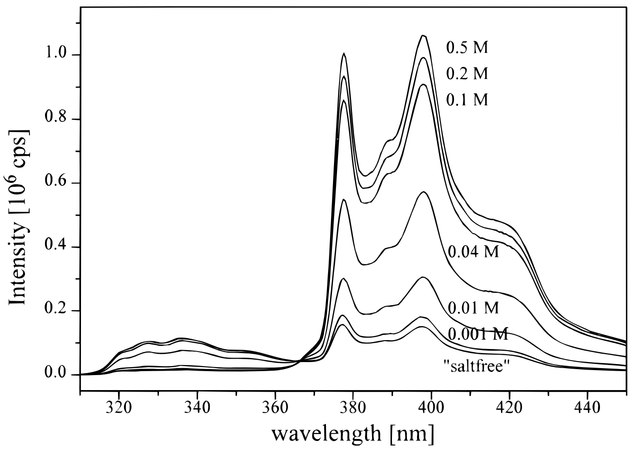

Figure 3. Fluorescence spectra of a mixture of AA_{45}-MMA_{20}-Py and AA_{40}-MMA_{20}-N (120 mg/L in water/NaOH) as a function of sodium chloride concentration.

remarkable. Even at low polymer concentrations (Figure 3), adding small amounts of sodium chloride leads to a pronounced increase in energy transfer. As shown in Figure 3, one observes a decrease in the naphthalene fluorescence intensity accompanied by an increase in the pyrene intensity, with a clear isoemissive point at 367 nm. The isoemissive point suggests that there is a change in the system involving only two discrete types of species, one favored in the absence of salt and the other favored by high ionic strength.

Salt effects on micelle formation for block copolymers with a polyelectrolyte block have been reported by several groups. Selb and Gallot[19c] examined micelle formation in quaternized derivatives of poly(styrene-*b*-4-vinylpyridine) and found few effects for high molecular weight polymers which were already associated at relatively low salt concentration (10^{-2} M), but for lower molecular weight species, salt promoted association. These authors conducted their experiments in a mixed solvent of water and methanol with LiBr as the added salt. Eisenberg and co-workers[3] used fluorescence probe experiments to show that the presence of salt lowered the cmc of poly(styrene-*b*-sodium acrylate) block copolymers. For two of these block copolymers with 6 and 23 styrene units, respectively, they demonstrated by light scattering that the aggregation number of their micelles increased significantly with increasing salt concentration.[32] Very recently, Baines et al.[33] used light-scattering and ultracentrifugation experiments to show that salt induced micellization of protonated poly(2-(dimethylamino)ethyl methacrylate-*b*-methyl methacrylate) block copolymers with 17 and 36 MMA units.

The presence of inorganic ions will have two effects on the solution. First, salt in the water can act as a precipitant for the PMMA block, making the continuous medium more polar and thereby a poorer solvent for this block. In addition, it will reduce the electrostatic repulsion between the hydrophilic blocks. Both effects will shift the equilibrium from a system rich in unimers to the formation of aggregates.

The limiting value of I_P/I_N at high salt concentration (0.5 M NaCl) increases with decreasing hydrophobic block length. At a polymer concentration of approximately 0.1 g/L, the value of I_P/I_N increases from 18 for MMA_{70} (prepared by method B, Figure 1) to 34 for MMA_{40} to 63 for MMA_{20}. The larger values of I_P/I_N reflect the higher local concentration in the smaller micelle cores: At similar degrees of functionalization of the block copolymers, the number of chromophores per volume of PMMA increases. This reduces the distance between donors and acceptors within the micelle core, and the energy transfer becomes more effective.

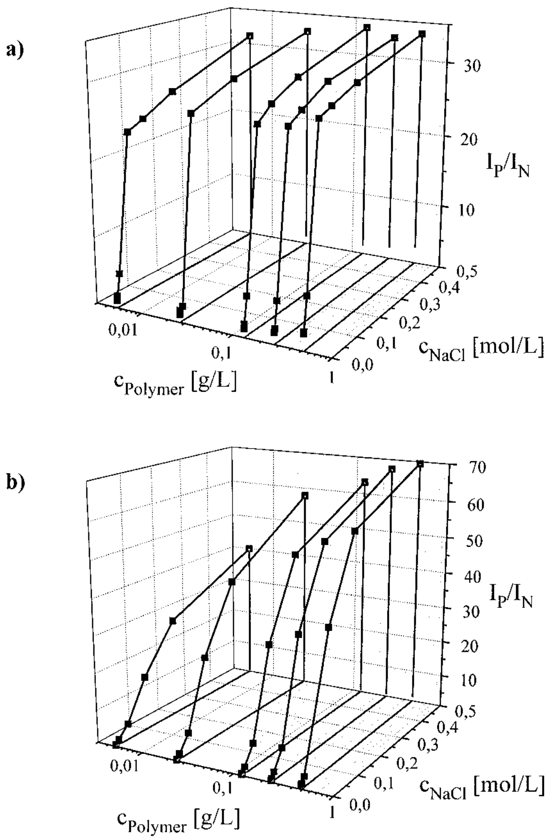

Figure 4. Ratio of pyrene-to-naphthalene fluorescence intensities for different polymer and salt concentrations. (a) AA_{40}-MMA_{40}-Py/AA_{35}-MMA_{35}-N, $c_{NaCl} = 0$, 10^{-3}, 10^{-2}, 0.05, 0.1, 0.2, 0.5 M; (b) AA_{45}-MMA_{20}-Py/AA_{40}-MMA_{20}-N, $c_{NaCl} = 0$, 10^{-3}, 10^{-2}, 0.04, 0.1, 0.2, 0.5 M.

Although the system is extremely sensitive to salt concentration, at each concentration of salt it remains rather insensitive to polymer concentration. This can be seen in Figure 4, where we present three-dimensional plots of I_P/I_N versus both NaCl and polymer concentration. In the case of AA_{45}-MMA_{20}-Py/AA_{40}-MMA_{20}-N (Figure 4b), the increase of I_P/I_N appears to be less pronounced at low polymer concentrations, but the apparent decrease of the I_P/I_N ratio is at least in part due to difficulties in distinguishing signal from noise for the very small naphthalene signal in these samples at low polymer concentration.

While the ratio I_P/I_N is a convenient measurement and automatically corrects for any fluctuations in the lamp intensity, we find that it does not give the most useful description of the extent of change in a system. More representative are the fractional changes in the pyrene or naphthalene signals, $(I_P - I_P^\circ)/(I_P^{max} - I_P^\circ)$ and $(I_N^\circ - I_N)/(I_N^\circ - I_N^{max})$, where I_P° and I_N° are the intensities in the absence of salt and I_P^{max} and I_N^{max} are the respective limiting intensities for complete association in the presence of high salt concentration. Mathematically we can write

$$x_{sig} = (I_P - I_P^\circ)/(I_P^{max} - I_P^\circ) = \alpha(I_N^\circ - I_N)/(I_P^{max} - I_P^\circ) \quad (1)$$

where x_{sig} represents the fractional change in the energy

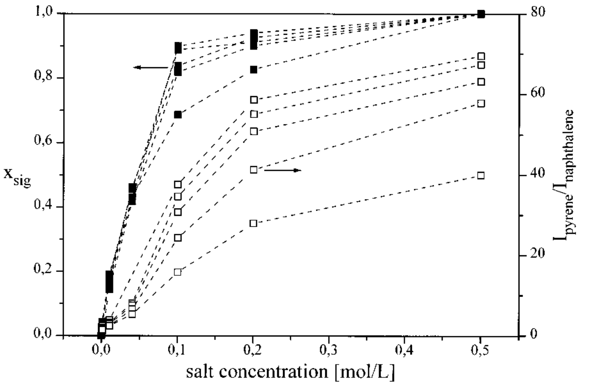

Figure 5. Comparison between plotting the data from Figure 4b as I_P/I_N and x_{sig} (eq 1), respectively, vs salt concentration.

transfer signal. In eq 1, α is the proportionality constant $(I_P - I_P°)/(I_N° - I_N)$ relating the increase in pyrene fluorescence to the decrease in naphthalene fluorescence. This leads to the following expression for I_P/I_N:

$$I_P/I_N = (\gamma + \alpha\beta x_{sig})/(1 - \beta x_{sig}) \qquad (2)$$

where $\beta = (I_P^{max} - I_P°)/(\alpha I_P°)$ takes account of incomplete NRET when all the N and Py are associated and γ is the ratio of pyrene-to-naphthalene fluorescence intensities in the absence of energy transfer $(I_P°/I_N°)$. For experimental convenience, we have chosen the ratio of N to Py in our experiments to give values of $\gamma = 1$ (see the Experimental Section).

To determine α in eq 2, we plot $(I_P - I_P°)$ vs $(I_N° - I_N)$, and α is the slope of the regression line. The value of β is obtained by taking I_P/I_N values from Figure 4 and plotting them against x_{sig} values calculated from the same original data with eq 1. We obtain β from the best fit of this plot to eq 2.[31] In this way we obtain values of $\alpha = 8.5$ and $\beta = 0.85$ for AA$_{45}$-MMA$_{20}$-Py/AA$_{40}$-MMA$_{20}$-N and $\alpha = 7.8$ and $\beta = 0.78$ for AA$_{40}$-MMA$_{40}$-Py/AA$_{35}$-MMA$_{35}$-N.

When we plot the data from Figure 4b as x_{sig} (see Figure 5), we see that addition of even small amounts of salt leads to a large increase in energy transfer. The I_P/I_N plot, on the other hand, de-emphasizes the changes that occur when small amounts of salt are added to the system. If we assume that x_{sig} is also a measure of the fraction of polymers which are associated, we see that 80% of the polymers in Figure 5 are associated in 0.1 M NaCl.

The effect of salt concentration on the aggregation behavior of the block copolymers can also be followed at higher concentration by ^{1}H NMR (Figure 6).[34] In pure D$_2$O all signals of AA$_{45}$-MMA$_{20}$-Py are somewhat broadened compared to the peaks of the same polymer in methanol, but the individual resonances are clearly apparent. When sodium chloride is added, the signals due to the PMMA block (shaded in Figure 6) decrease significantly, because the exchange between different chemical environments is slowed down by aggregation. In contrast, the signals of the poly(acrylic acid) block and of the initiator fragment remain almost unaffected. When chloroform, a selective solvent for the hydrophobic block, is then added to the sample tube, the micellar core becomes more mobile again. The PMMA signals reappear in the spectrum.

Additional evidence about the aggregation induced by salt is given by light-scattering measurements. The light-scattering intensity at 90° from a solution of AA$_{45}$-MMA$_{20}$-Py/AA$_{40}$-MMA$_{20}$-N increases by a factor of two by changing the salt concentration from 0.05 to 0.5 M NaCl. In addition, from dynamic light scattering one can deduce an increase of the hydrodynamic radius (R_h) of the micelles with increasing NaCl concentration, from 5.4 nm (0.05 M) to 6.6 nm (0.1 M) to 7.0 nm (0.5 M). Although the hydrodynamic radius is primarily sensitive to the dimensions of the micelle corona, salt would not be expected to lead to stretching of the polyelectrolyte corona chains. This growth in R_h must be due to an increase in the aggregation number of the micelles. Here, however, in contrast to the behavior of block copolymer with 70 MMA units, the correlation functions (Figure 7) obtained from dynamic light scattering do not correspond to a simple exponential decay. They can be fitted with a sum of two exponential functions. The faster process corresponds to species with the dimensions of the micelles, whereas the slower process (which makes a decreasing contribution to the signal with increasing salt concentration) corresponds to a species with an R_h of approximately 60 nm with a large q-dependence. This process is likely associated with the formation of large loose aggregates of block copolymers, which may form through association of the hydrophobic groups (from the initiator fragment) at the hydrophilic chain ends. Further work is needed to characterize these structures.

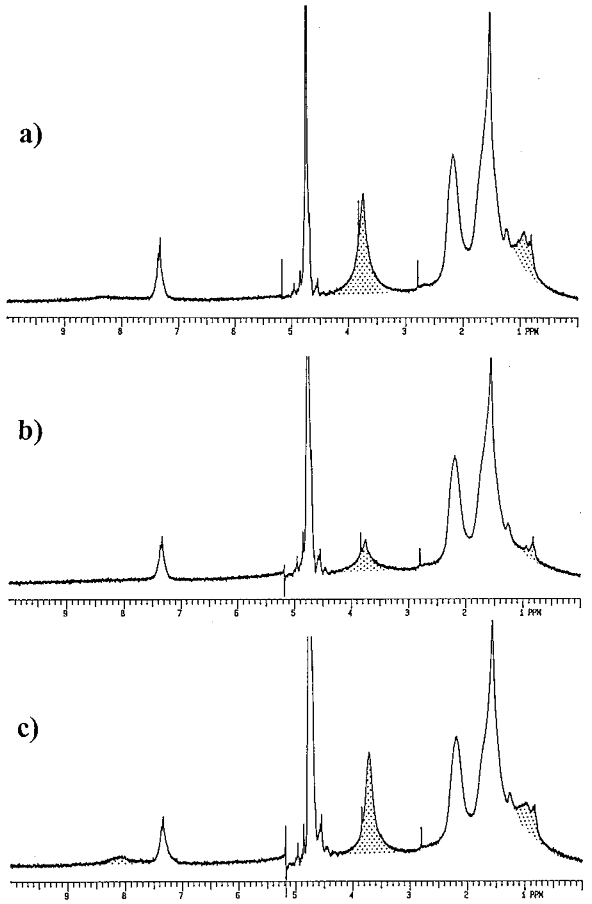

Figure 6. ^{1}H NMR spectra (room temperature, absolute intensity mode) of AA$_{45}$-MMA$_{20}$-Py (20 g/L) (a) in deuterated water, (b) in deuterated water with 0.2 M NaCl, and (c) in deuterated water with 0.2 M NaCl and a trace of deuterated chloroform. δ (ppm) = 0.9 (C−CH_3); 1.5 (CH_2); 2.2 (CH(COOH)); 3.7 (-COOCH_3); 7.3 (phenyl); 8.1 (pyrene). Signals assigned to protons of the PMMA block are shaded.

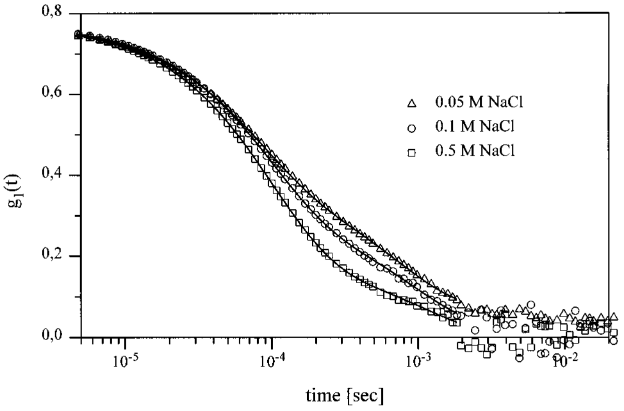

Figure 7. Correlation functions from dynamic light-scattering measurements at 90° for AA_{45}-MMA_{20}-Py/AA_{40}-MMA_{20}-N (2 g/L) with sodium chloride concentrations of 0.05 M (triangles), 0.1 M (circles), and 0.5 M (squares). Connected lines are obtained by fitting the data with a sum of two exponentials.

Chain Exchange in the Presence of Salt. If salt strongly influences the solubility of the two block copolymers with 20 and 40 MMA units, one can expect that it also affects the exchange kinetics of chains between micelles for these polymers. To examine this question, we prepared various separate micellar solutions, at different salt concentrations, of the naphthalene- and pyrene-labeled polymers (cf., Figure 1, method A) with polymer concentrations of 16 mg/L (pyrene-labeled) and 80 mg/L (naphthalene-labeled). The two separate solutions were mixed in a 1:1 ratio at $t = 0$ as to give—once again—solutions with a ratio of N- to Py-labeled polymer of 5:1. Fluorescence spectra of these solutions were recorded after different time intervals. Values of I_P/I_N, plotted in Figure 8, increase with time. This increase is quite slow, and even after 1 day, the limiting values for I_P/I_N (see Figure 4) are not reached.

Several features of this plot require explanation. In Figure 8a, for AA_{40}-MMA_{40}-Py/AA_{35}-MMA_{35}-N, one sees that the rate of increase of I_P/I_N is faster in the presence of 0.04 M and 0.1 M salt than in 0.4 M salt. In Figure 8b, for AA_{45}-MMA_{20}-Py/AA_{40}-MMA_{20}-N, the effect of salt seems to be the reverse, with the largest change in I_P/I_N occurring for 0.4 M salt. The plots in Figure 8 are influenced not only by the effect of salt concentration on the rate of polymer exchange between micelles but also by the effect of salt concentration on the limiting value of I_P/I_N. To clarify the effect of salt on the exchange process, we have to take into account the effect of salt on the limiting extent of micellization. One way that this could be done would be to use the values of the individual component intensities and calculate the fractional change in analogy with eq 1:

$$x_{\mathrm{sig}}^* = (I_P - I_P^\circ)/(I_p^{\mathrm{eq}} - I_P^\circ) \tag{3}$$

where instead of $I_P^{\max}$ we have to use the limiting pyrene fluorescence intensity for complete equilibration of the sample at the particular salt concentration, I_P^{eq}. Calculating x_{sig}^* in this way has the disadvantage that changes in the intensity of the excitation source during the time of the experiment would influence the data. In addition, we do not have absolute values of I_p^{eq}.[35] For this reason, we calculate an apparent $x_{\mathrm{sig}}^{\mathrm{app}}$ from the I_P/I_N values in Figure 8 using eq 2, where $I_p^{\max}$ is the limiting fluorescence intensity in the presence of high salt concentration.

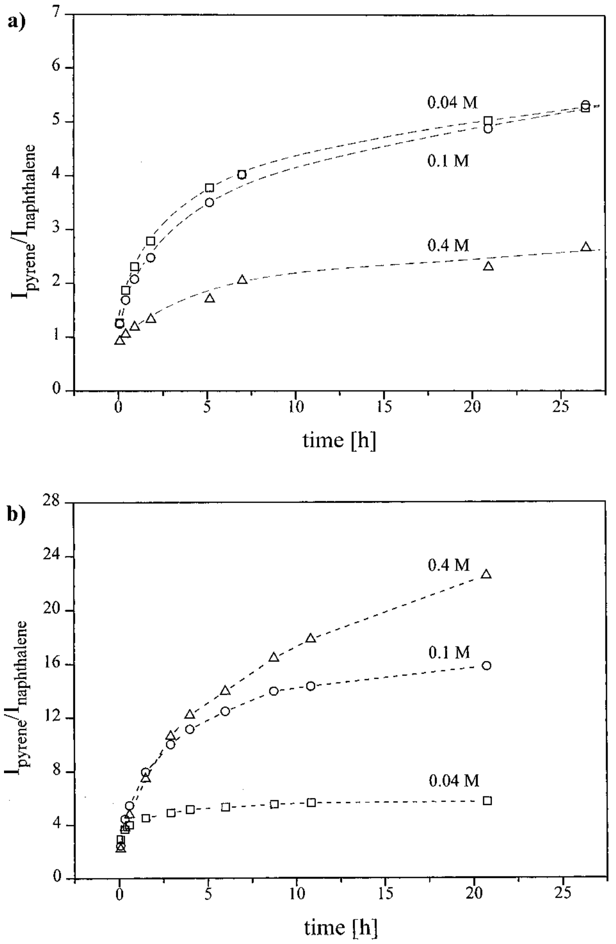

Figure 8. Time-dependent change of the ratio I_P/I_N in the presence of different NaCl concentrations at room temperature (a) for AA_{40}-MMA_{40}-Py/AA_{35}-MMA_{35}-N and (b) for AA_{45}-MMA_{20}-Py/AA_{40}-MMA_{20}-N. The concentrations were 40 mg/L for the naphthalene-labeled polymer and 8 mg/L for the pyrene-labeled polymer.

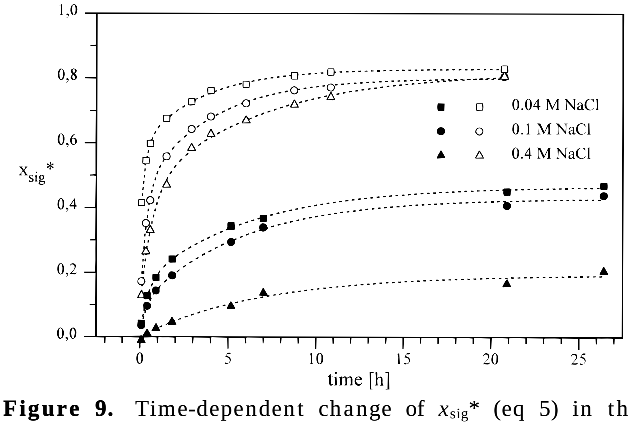

Figure 9. Time-dependent change of x_{sig}^* (eq 5) in the presence of different NaCl concentrations at room temperature for AA_{40}-MMA_{40}-Py/AA_{35}-MMA_{35}-N (filled symbols) and AA_{45}-MMA_{20}-Py/AA_{40}-MMA_{20}-N (open symbols).

To proceed, we re-express eq 3 as

$$x_{\mathrm{sig}}^* = (I_P - I_P^\circ)/(I_p^{\max} - I_P^\circ)\cdot(I_p^{\max} - I_P^\circ)/(I_p^{\mathrm{eq}} - I_P^\circ) \tag{4}$$

The first ratio on the right hand side of eq 4 is the apparent $x_{\mathrm{sig}}^{\mathrm{app}}$. The second term is the inverse of x_{sig}, and values for this quantity are calculated from the data in Figure 4. Hence, eq 4 can be written as

$$x_{\mathrm{sig}}^* = x_{\mathrm{sig}}^{\mathrm{app}}/x_{\mathrm{sig}} \tag{5}$$

The resulting plot of the fraction of exchange vs. time is shown in Figure 9. Here we see that the exchange process begins rapidly at all salt concentrations for the polymer with the MMA_{20} block and that the extent of exchange attained after 1 day is quite high. In the case of the polymer with the MMA_{40} block, the increase is much slower, and even after 20 h, the system is still far from full exchange.

It is important to realize that we cannot equate the extent of energy transfer with the extent of block copolymer exchange in the system. Because of the small size of the micelle core and because of the possibility of N−N hopping preceding energy transfer to Py, entry of a single Py-labeled polymer into an otherwise N-labeled micelle will lead to a high efficiency of energy transfer for all of the N-groups in the micelle. As a consequence, the increase in energy transfer caused by an exchanging chain will not be the same at the beginning and at the end of the equilibration process.

Conclusion

The association behavior of poly(acrylic acid sodium salt-*b*-methyl methacrylate) block copolymers in water strongly depends on the hydrophobic block length but is almost unaffected by polymer concentration. Polymers with 70 MMA units in the insoluble block form micelles at even the lowest concentrations that can be detected (0.1 mg/L). Energy transfer measurements on block copolymer pairs labeled with donor (naphthalene) and acceptor (pyrene) groups on the respective chain ends show that no detectable polymer exchange occurs on the time scale of weeks and that the direct dissolution in water seems to take place by a break up of the polymer grains into colloidal particles. Energy transfer measurements on aqueous solutions of block copolymers with shorter PMMA blocks (MMA_{20} and MMA_{40}) indicate that these systems come rapidly to equilibrium in the absence of added salt. Our results suggest that these two polymer species are mainly present as unassociated unimers in pure water. An increase of energy transfer is observed as the polymer concentration is increased, but this is due primarily to *radiative* energy transfer. None of the block copolymers exhibit the type of concentration-dependent change in energy transfer expected for a sharp transition from unimers to micelles. We conclude that micelle formation in this system does not exhibit a clear cmc.

In this system, polymer association is strongly promoted by adding salt to the solution. Labeled pairs of the smaller block copolymers in aqueous solution (with MMA_{20} and MMA_{40}) show a pronounced increase in energy transfer in the presence of sodium chloride. The presence of salt also slows down the rate of exchange of polymer molecules between micelles.

Acknowledgment. This work was supported by the Federal Ministry of Research and Technology of Germany (BMBF, contract no. 03N30043). M.A.W. would like to thank the Alexander von Humboldt Foundation for support of his stay in Germany.

References and Notes

(1) Wilhelm, M.; Zhao, C.-L.; Wang, Y.; Xu, R.; Winnik, M. A.; Mura, J.-L.; Riess, G.; Croucher, M. D. *Macromolecules* **1991**, *24*, 1033−1040.

(2) Astafieva, I.; Zhong, X. F.; Eisenberg, A. *Macromolecules* **1993**, *26*, 7339−7352.

(3) Astafieva, I.; Khougaz, K.; Eisenberg, A. *Macromolecules* **1995**, *27*, 7127−7134.

(4) (a) Alexandridis, P.; Holzwarth, J. F.; Hatton, T. A. *Macromolecules* **1994**, *27*, 2414-2425. (b) Alexandridis, P.; Hatton, T. A. *Colloids Surf., A* **1995**, *96*, 1−46.

(5) Kabanov, A. V.; Nazarova, I. R.; Astafieva, I. V.; Batrakova, E. V.; Alakhov, V. Y.; Yaroslavov, A. A.; Kabanov, V. A. *Macromolecules* **1995**, *28*, 2303−2314.

(6) Holland, R. J.; Parker, E. J.; Guiney, K.; Zeld, F. R. *J. Phys. Chem.* **1995**, *99*, 11981−11988.

(7) Jada, A.; Siffert, B.; Riess, G. *Colloids Surf., A* **1993**, *75*, 203−209.

(8) Caldérara, F.; Hruska, Z.; Hurtrez, G.; Lerch, J.-P.; Nugay, T.; Riess, G. *Macromolecules* **1994**, *27*, 1210−1215.

(9) Procházka, K.; Kiserow, D.; Ramireddy, C.; Tuzar, Z.; Munk, P.; Webber, S. E. *Macromolecules* **1992**, *25*, 454−460.

(10) Wang, Y.; Kausch, C. M.; Chun, M.; Quirk, R. P.; Mattice, W. L. *Macromolecules* **1995**, *28*, 904−911.

(11) Wang, Y.; Balaji, R.; Quirk, R. P.; Mattice, W. L. *Polym. Bull.* **1992**, *28*, 333−338.

(12) Munk, P.; Ramireddy, C.; Tian, M.; Webber, S. E.; Procházka, K.; Tuzar, Z. *Makromol. Chem., Macromol. Symp.* **1992**, *58*, 195−199.

(13) Tian, M.; Qin, A.; Ramireddy, C.; Webber, S. E.; Munk, P.; Tuzar, Z.; Procházka, K. *Langmuir* **1993**, *9*, 1741−1748.

(14) Elias, H.-G.; Bareiss, R. *Chimia* **1967**, *21*, 53−65.

(15) Selb, J.; Gallot, Y. *Makromol. Chem.* **1980**, *181*, 809−822.

(16) Chan, J.; Fox, S.; Kiserow, D.; Ramireddy, C.; Munk, P.; Webber, S. E. *Macromolecules* **1993**, *26*, 7016−7023.

(17) Tuzar, Z.; Webber, S. E.; Ramireddy, C.; Munk, P. *Polym. Prepr.* **1991**, *32* (1), 525-526.

(18) Qin, A.; Tian, M.; Ramireddy, C.; Webber, S. E.; Munk, P.; Tuzar, Z. *Macromolecules* **1994**, *27*, 120−126.

(19) (a) Selb, J.; Gallot, Y. *Makromol. Chem.* **1980**, *181*, 2605−2624. (b) Selb, J.; Gallot, Y. *Makromol. Chem.* **1981**, *182*, 1491−1511. (c) Selb, J.; Gallot, Y. *Makromol. Chem.* **1981**, *182*, 1513−1524.

(20) Xu, R.; Hu, Y.; Winnik, M. A.; Riess, G.; Croucher, M. D. *J. Chromatogr.* **1991**, *547*, 434−438.

(21) See, for example: Procházka, K.; Martin, T. J.; Munk, P.; Webber, S. E. *Macromolecules* **1996**, *29*, 6518−6525.

(22) (a) Turro, N. J. *Modern Molecular Photochemistry*; University Science Books: Mill Valley, CA, 1991; p 296 ff. (b) Hoppe, Lohmann, Markl, Ziegler, Eds. *Biophysik*, 2nd ed.; Springer: Berlin, 1982; p 275 ff. (c) Berlman, I. B. *Energy Transfer Parameters of Aromatic Compounds*; Academic Press: New York, 1973.

(23) Varshney, S. K.; Jacobs, C.; Hautekeer, J.-P.; Bayard, P.; Jerôme, R.; Fayt, R.; Teyssié, P. *Macromolecules* **1991**, *24*, 4997−5000.

(24) (a) Rudolph, J.; Patzsch, J.; Meyer, W. H.; Wegner, G. *Acta Polym.* **1993**, *44*, 230−237. (b) Rudolph, J. Ph.D. Thesis, Mainz, 1994.

(25) Al-Takrity, E. T. B.; Jenkins, A. D.; Walton, D. R. M. *Makromol. Chem.* **1990**, *191*, 3069−3072.

(26) Allen, R. D.; Long, T. E.; McGrath, J. E. *Polym. Bull.* **1986**, *15*, 127−134.

(27) Duhamel, J.; Yekta, A.; Hu, Y. Z.; Winnik, M. A. *Macromolecules* **1992**, *25*, 7024−7030.

(28) (a) Lehmann, U.; Köhler, W.; Albrecht, W. *Macromolecules* **1996**, *29*, 3212−3215. (b) Lehmann, U. Ph.D. Thesis, Mainz, 1996.

(29) Staudinger, H. *Die hochmolekularen organischen Verbindungen−Kautschuk und Cellulose*; Springer: Berlin, 1932; p 371.

(30) Mandel, M. Polyelectrolytes. In *Encyclopedia of Polymer Science and Engineering*; Mark, Bikales, Overberger, Menges, Eds.; John Wiley & Sons: New York, 1988; Vol. 11, pp 739−829.

(31) Rager, T. Ph.D. Thesis, Mainz, 1997.

(32) Khougaz, K.; Astafieva, I.; Eisenberg, A. *Macromolecules* **1995**, *28*, 7135−7147.

(33) (a) Baines, F. L.; Billingham, N. C.; Armes, S. P. *Macromolecules* **1996**, *29*, 3416−3420. (b) Baines, F. L.; Armes, S. P.; Billingham, C.; Tuzar, Z. *Macromolecules* **1996**, *29*, 8151−8159.

(34) Kriz, J.; Masar, B.; Pospisil, H.; Plestil, J.; Tuzar, Z.; Kiselev, M. A. *Macromolecules* **1996**, *29*, 7853−7858.

(35) Values of I_P^{eq} could be taken from the original data of Figure 4 if the solution concentrations and excitation source intensities were identical.

MA961866L